J Wood Sci (2006) 52:302–310
DOI 10.1007/s10086-005-0766-z

ORIGINAL ARTICLE

Tamami Kawasaki · Min Zhang · Qian Wang
Kohei Komatsu · Shuichi Kawai

Elastic moduli and stiffness optimization in four-point bending of wood-based sandwich panel for use as structural insulated walls and floors

Received: February 18, 2005 / Accepted: September 16, 2005 / Published online: March 2, 2006

Abstract Several wood-based sandwich panels with low-density fiberboard core were developed for structural insulated walls and floors, with different face material, panel thickness, and core density. The elastic moduli with and without shear effect (E_L, E_0) and shear modulus (G_b) were evaluated in four-point bending. Generally, the stiffer face, thicker panel, and higher core density were advantageous in flexural and shear rigidity for structural use, but the weight control was critical for insulation. Therefore, optimum designs of some virtual sandwich structures were analyzed for bending stiffness in relation to weight for fixed core densities, considering the manufactured-panel designs. As a result, the plywood-faced sandwich panel with a panel thickness of 95 mm (PSW-T100), with insulation performance that had been previously confirmed, was most advantageous at a panel density of 430 kg/m^3, showing the highest flexural rigidity ($E_L I = 13 \times 10^{-6}$ GNm^2) among these panels, where E_L, E_0, and G_b were 3.5, 5.5, and 0.038 GN/m^2, respectively. The panel was found to be closest to the optimum design, which meant that its core and face thickness were optimum for stiffness with minimum density. The panel also provided enough internal bond strength and an excellent dimensional stability. The panel was the most feasible for structural insulation use with the weight-saving structure.

Key words Bending property · Wood-based sandwich panel · Low-density fiberboard · Structural insulation wall/floor · Optimum design analysis

T. Kawasaki (✉) · M. Zhang · S. Kawai
Laboratory of Sustainable Materials, Research Institute for Sustainable Humanosphere, Kyoto University, Uji 611-0011, Japan
Tel. +81-774-38-3677; Fax +81-774-38-3678
e-mail: tkawasaki@rish.kyoto-u.ac.jp

K. Komatsu
Laboratory of Structural Function, Research Institute for Sustainable Humanosphere, Kyoto University, Uji 611-0011, Japan

Q. Wang
Hokushin Co., Kishiwada 596-8521, Japan

Introduction

There is a dire need for more effective measures for sustaining comfortable temperatures in living environments because of the emerging trend of global warming. Insulation materials are therefore required to demonstrate higher performance so that temperatures in residences can be moderated against the severe temperature changes that occur diurnally and seasonally.

The current commercial insulators for houses, such as plastic foams and mineral wools, are inferior to the warmth-keeping property of low-density fiberboards. Low-density fiberboard, the mechanical properties of which were improved in a previous study,[1] is a promising insulation material that provides low thermal conductivity. This characteristic of the fiberboards made the most of the wood resource, which came from the species of trees that have survived severe climate changes throughout the earth's history.

Structural insulated panels with a plastic foam core are currently used in a sandwich structure with face materials of oriented strand board (OSB).[2] Wood-based sandwich panel had been behind the development of many industrial sandwich structures for a long time.[3] Following the studies of wood-based sandwich beam[4] and panels,[5,6] we have developed plywood-faced sandwich (PSW)[7] panels with low-density fiberboard for use as wood-based structural insulated walls/floors. We showed that PSW had characteristics of well-balanced thermal insulation and warmth-keeping properties,[8] as well as the feasibility for structural use[7] by evaluating the in-plane shear modulus, which is required in structural calculations of walls/floors.

In the present work, some wood-based sandwich panels with low-density fiberboard were manufactured with different thickness, core density, and face materials. A four-point out-plane bending test was conducted, and the elastic and shear moduli were determined, which are also important for structural calculations. The flexural rigidities of these panels are discussed.

Weight control is critical for insulation use, because density plays a dominant role in insulation performance. The optimization of sandwich structures between stiffness and weight and some stiffness analysis have been considered by a number of authors,[3,9–16] but the optimization of wood-based sandwich panels, and particularly under concentrated two-point loading, appears to be much less well understood. Therefore, the optimum designs of some virtual wood-based sandwich structures were analyzed by considering the designs of the manufactured panels.

Experimental

Face and core materials

For core materials, fiber from lauan (*Shorea* spp.) was prepared, which was commercially produced using a pressurized double disk refiner (PDDR) (Hokushin). For face materials, plywood (PW) and medium-density fiberboard (MDF) were prepared. The PW was commercially produced weatherproof and boil-proof plywood (type special[17]) (Ishinomaki Plywood) with a thickness of 9mm and a density of 600kg/m^3, and consisted of three plies of 3-mm layers of Japanese larch (*Larix gmelini* Gordon). The MDF was commercially produced from hardwood fiber using an adhesive of melamine–urea–formaldehyde resin (Hokushin) with a thickness of 9mm and a density of 700kg/m^3.

Manufacture of sandwich panels

Six types of wood-based sandwich panels with fiberboard core were manufactured as listed in Table 1; plywood-faced sandwich panels with a target thickness of 100mm (PSW-T100) at three density levels (types 1–3), and plywood-faced sandwich panels with a target thickness of 50mm (PSW-T50) at two density levels (types 4, 5), and a MDF-faced sandwich panel with a target thickness of 100mm (MSW-T100) (type 6).

The manufacturing procedure of sandwich panels was as follows. The fiber was put into a cyclic-tube-type blender and the commercial adhesive of polymeric methylene diphenyl diisocyanate (MDI) (Mitsui Takeda Chemical) was sprayed into the fiber using a spray gun during the cycle. The resin content was 10% solid resin of MDI based on the oven-dried fiber weight. The fiber was formed into fiber mats in a size of 0.26 (width) × 1.6m (length) using a forming box by hand forming. Some thicker fiber mats for higher density panels were preliminarily pressed to obtain adequate mat heights using a cold pressing machine. All face materials were prepared in a size of 0.26 (width) × 1.6m (length). Before pressing, MDI adhesive (UL-4811, Gun-ei Chemical) was spread on the back side of each face material at approximately 80g/m^2 on solid basis using a hard plastic hand roller. The face materials were then symmetrically placed on the top and bottom surfaces of each fiber mat so that the grain of the plywood surface was parallel to the panel length direction.

The assembled mats were pressed using a continuous pressing machine with steam injection on both sides.[18] The pressing space size of the machine was 300mm in width, 100mm in height, and 1500mm in length. The mats for PSW-T100 and MSW-T100 were pressed one by one whereas two mats for PSW-T50 were piled up and pressed together. The assembled mats were put into the pressing space between the press platens heated to 170°C, moved by a steel belt at a velocity of 1m/min, and then heated by steam (160°C) injected from both sides of three pairs of steam valves near the entrance of the machine for approximately 2min. After the injection the belt was stopped, and the mat was held and pressed for approximately 10min to obtain sufficient bonding. By moving the belt again, the sandwich panels were obtained from the exit of the pressing space and then stabilized to an air-dried condition in a well-ventilated room for over 2 weeks. One piece of sandwich panel for each type was then obtained in a size of 0.26 (width) ×1.6m (length).

Property testing

A four-point bending test was conducted for PSW-T100, PSW-T50, and MSW-T100, according to the out-plane bending test in JIS (Japanese Industrial Standard) A 1414,[19] with modifications in specimen width and length. Three beam specimens, 0.05m in width (b) and 1.6m in length (l), were taken from the center of each panel. As shown in

Table 1. Experimental geometric data of the manufactured sandwich panels

No.	Specimen	Face	ρ_{sw} (kg/m^3)	ρ_c (kg/m^3)	ρ_f (kg/m^3)	c (m)	f (m)	h (m)	W (kg)
1	PSW-T100	PW	320	250	600	0.078	0.009	0.096	2.28
2			350	300	600	0.077	0.009	0.095	2.54
3			430	390	600	0.077	0.009	0.095	3.09
4	PSW-T50		430	350	600	0.035	0.009	0.053	1.74
5			480	400	600	0.026	0.009	0.044	1.58
6	MSW-T100	MDF	380	330	700	0.077	0.009	0.095	2.71

The data are average values of the specimens for the out-plane bending test. ρ_{SW}, Panel density; ρ_c, core density; ρ_f, face density; c, core thickness; f, face thickness for each sheet; h, panel thickness; W, weight of a sandwich beam between the supporting points ($W = bhL$); $b = 0.05$m (width), $L = 1.5$m (whole span). PW, plywood; MDF, medium-density fiberboard

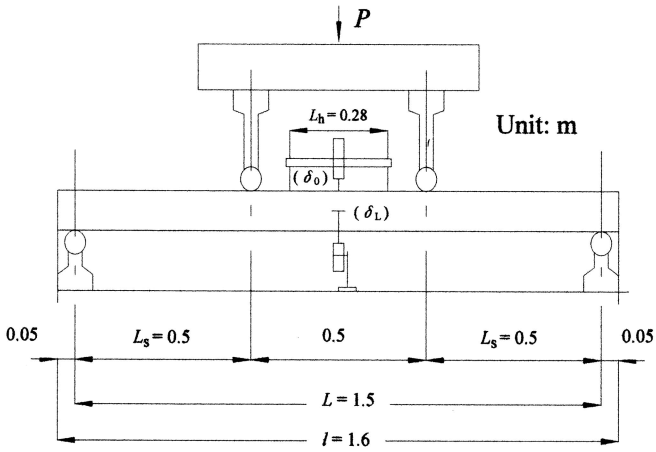

Fig. 1. Four-point bending test. P, load; L, whole span; L_h, distance between the measuring points for δ_0; L_s, span subjected to shear deformation; l, length of specimen; δ_L, deflection at mid span; δ_0, relative deflection between loading points

Fig. 1, the whole span length (L) was 1.5 m, and two loading points were set to divide the span into three equal parts of 0.5 m each. The tests for PSW-T100 and PSW-T50 were conducted in a direction parallel to the grain of the plywood surface. The load–deflection curve was recorded. The deflection at mid span (δ_L) was measured to determine the equivalent apparent elastic modulus (E_L) including shear deformation effect (Eq. 1). A relative deflection between the loading points (δ_0) was measured (the distance of the measuring points was $L_h = 0.28$ m) to determine the equivalent pure elastic modulus (E_0) excluding shear deformation effect in pure bending (Eq. 2).

$$E_L = \frac{\Delta P}{\Delta \delta_L} \frac{\left(3L_s L^2 - 4L_s^3\right)}{48I} \tag{1}$$

$$E_0 = \frac{\Delta P}{\Delta \delta_0} \frac{\left(L L_h^2\right)}{48I} \tag{2}$$

where L_s is the span subjected to the shear deformation (L_s = 0.5 m), and I is the moment of inertia for a rectangular cross section of a beam. The slopes $\Delta P/\Delta\delta_L$ and $\Delta P/\Delta\delta_0$ are defined from the linear portion of the relations between the load P and the deflections δ_L and δ_0, respectively. From the E_L and E_0 values (Eqs. 3 and 4), the equivalent shear modulus in bending (G_b) was calculated from Eq. 5:

$$\delta_L = \frac{P\left(3L_s L^2 - 4L_s^3\right)}{48 E_L I} \tag{3}$$

$$\delta_L = \frac{P\left(3L_s L^2 - 4L_s^3\right)}{48 E_0 I} + \frac{\kappa P L_s}{2 G_b A} \tag{4}$$

$$G_b = \frac{2\kappa h^2 E_0 E_L}{\left(E_0 - E_L\right)\left(3L^2 - 4L_s^2\right)} \tag{5}$$

where the value κ is a constant for a rectangular beam ($\kappa = 1.2$), and h is the panel thickness.

Generally, the elastic modulus of a sandwich structure (E_T) can be calculated from the elastic modulus of the core (E_c) and face materials (E_f) using the composite theory (Eq. 6).

$$E_T = \frac{E_c c^3 - E_f\left(h^3 - c^3\right)}{h^3} \tag{6}$$

where the value c is the core thickness.

For simulation of E_T values of the sandwich panels, the modulus of elasticity (MOE) of face materials and fiberboards (FB) was determined as follows. The FB boards were manufactured at densities of 280, 360, and 460 kg/m^3, similarly to the core densities, with a thickness of 12 mm using the same fiber prepared in the same manner with modifications to the forming and pressing method: the fiber was formed using a forming machine and pressed for 4 min using a hot-pressing machine. One piece of FB was obtained (0.36 × 0.37 m in area) for each density level, and then stabilized to an air-dried condition in a well-ventilated room for over 2 weeks.

A central-load bending test was conducted on PW, MDF, and FB, according to Japanese Agricultural Standard (JAS) for structural plywood[17] and JIS A 5905,[20] with a modification of the specimen width in the dimensions (width × length) for PW (0.05 × 0.29 m), for MDF (0.05 × 0.23 m), and for FB (0.03 × 0.23 m). Five specimens were prepared from each board. The test span was 0.18 m for all specimens. The test for PW was conducted in directions that were parallel and perpendicular to the grain of the plywood surface.

The MOE was determined for each specimen. The MOE values of faces and FB (E_{FB}) were substituted for E_f and E_c in Eq. 6, respectively, for the simulation of the E_T values, which were compared with the E_0 values. The MOR was also recorded for each specimen.

An internal bond (IB) test was conducted on four specimens (0.05 m square × thickness) from each panel of PSW-T100 and FB. Thickness swelling (TS) and water absorption (WA) were tested on four specimens (0.05 m square × thickness) from each panel of PSW-T100, PSW-T50, and MSW-T100. The thickness and weight of the specimens after water soaking at 20°C for 24 h were measured, and the TS and WA were then calculated. These tests were conducted according to the test for veneer-overlaid particleboard in JIS A 5908.[21] The density profiles of the core material in the thickness direction of the PSW-T100 panels were flat.[8]

Results and discussion

Elastic and shear moduli

Table 2 shows the experimental material constants in the bending of the manufactured sandwich panels and these results are shown plotted against panel density in Fig. 2. As shown in Fig. 2A, the $E_L I$ (apparent flexural rigidity) values of PSW-T100 panels at the average densities of 350 and

Table 2. Experimental material constants in out-plane bending of the manufactured sandwich panels

No.	Specimen	ρ_{SW} (kg/m^3)	P/δ_L (MN/m)	E_LI ($\times 10^{-6}$ GNm^2)	E_L (GN/m^2)	E_0I ($\times 10^{-6}$ GNm^2)	E_0 (GN/m^2)	G_bA ($\times 10^{-3}$ GN)	G_b (GN/m^2)	E_L/E_0
1	PSW-T100	320	0.071	4.2	1.2	19	5.1	0.028	0.0060	0.24
2		350	0.18	11	3.0	22	6.2	0.11	0.022	0.48
3		430	0.21	13	3.5	20	5.5	0.18	0.038	0.65
4	PSW-T50	430	0.067	4.0	6.4	5.1	8.1	0.10	0.036	0.79
5		480	0.042	2.5	7.4	2.7	7.8	0.25	0.114	0.95
6	MSW-T100	380	0.086	5.1	1.4	6.5	1.8	0.13	0.026	0.79

The data are average values of the specimens for the bending test. P/δ_L, Stiffness; E_LI, apparent flexural rigidity; E_L, apparent elastic modulus; E_0I, pure flexural rigidity; E_0, pure elastic modulus; G_bA, shear rigidity; G_b, shear modulus

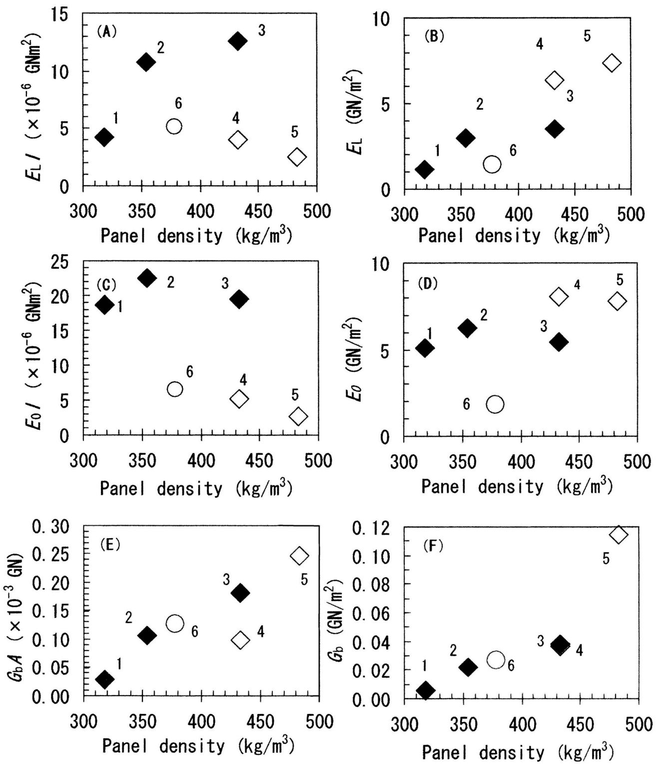

Fig. 2A–F. Bending material constants of manufactured sandwich panels. **A** E_LI, flexural rigidity; **B** E_L, elastic modulus; **C** E_0I, pure flexural rigidity; **D** E_0, pure elastic modulus; **E** G_bA, shear rigidity; **F** G_b, shear modulus. *Numbers*, models of the sandwich panels (*1–3*, *filled diamonds*, PSW-T100; *4*, *5*, *open diamonds*, PSW-T50; *6*, *open circle*, MSW-T100, see Table 1)

430 kg/m^3 (nos. 2 and 3) were more than twice (11 and 13 $\times$ 10^{-6} GNm^2) those of the other panels.

The E_LI values were related to two main components: pure flexural rigidity (E_0I) and shear rigidity (G_bA). The E_0I values differed due to the different thickness or face materials (Fig. 2C), whereas the G_bA values generally depended on panel density (Fig. 2E). The trend in the E_LI values was similar to that in the E_0I values, although the E_LI values decreased due to the shear deformation effect. The decreasing trend was remarkable for a low panel density.

The E_L (apparent elastic modulus) values generally depended on panel density (Fig. 2B). The E_0 (pure elastic modulus) values varied more due to the difference of face material than that of thickness (Fig. 2D). As a result, the E_L/E_0 ratios of the sandwich panels were generally close to 1 at high density and decreased at low density (Table 2). Because the G_b (shear modulus) values strongly depended on panel density (Fig. 2F), the shear deformation effect on the E_L values increased for low panel density.

A reverse trend was found in the panels of PSW-T100 and PSW-T50 between the E_LI and E_L values: the E_LI value of the PSW-T100 panel (no. 3) was approximately three times that of the PSW-T50 panel (no. 4) at the same panel density (Fig. 2A), whereas the E_L value of the PSW-T100 panel (no. 3) was approximately half that of the PSW-T50 panel (no. 4) in Fig. 2B. This was because the thickness factor had a great effect on the E_LI value.

The panel thickness of PSW-T50 panels was half that of the PSW-T100 panels, whereas the face thickness was the same. Therefore, the face-to-panel thickness ratio of PSW-T50 panels was twice that of PSW-T100 panels, which was advantageous for increasing the E_L value of PSW-T50 panels. However, the advantage was cancelled by the decreasing E_LI value, where the thickness was raised to the third power.

As shown in Fig. 2A, the E_LI value of MSW-T100 panel (no. 6) was less than half that of the PSW-T100 panel (no. 3) and somewhat more than that of the PSW-T50 panel (no. 4), whereas the E_L value of the MSW-T100 was less than those of panel nos. 3 and 4 (Fig. 2B) at a similar panel density. The effect of face material was clearly observed on the E_0I values (Fig. 2C), but not on the G_bA values (Fig. 2E). This was because the difference of MOE values between the face materials had a great effect on the E_0 values.

The average MOE values of PW in the parallel and perpendicular directions were 13 and 0.70 GN/m^2, respectively, at the average density of 600 kg/m^3. The average MOE value of MDF was 3.0 GN/m^2 at an average density of 700 kg/m^3. The MOE of PW in the parallel direction was approximately four times that of MDF.

The PSW-T100 panel (no. 1) provided a high E_0 value, similar to the other PSW-T100 panels (nos. 2 and 3). However, the low density was disadvantageous in the G_b value over the other panels (Fig. 2F), which caused the E_L value to be reduced (Fig. 2B). The higher density of the PSW-T50 panel (no. 5) was advantageous in providing a higher G_b value than those of the other panels, but the effect was not significant on the E_0 and E_L values. From the above results, the structure of PSW-T100 panel (no. 3) was the most effective construction to improve the $E_L I$ values among these sandwich panels.

For reference, the standard value of MOE for veneer-overlaid particleboard is 4.5 GN/m^2 according to JIS A 5908.[21] The E_0 values (5.1–8.1 GN/m^2) of PSW-T100 and PSW-T50 panels (nos. 1–5) and the E_L values (6.4 and 7.4 GN/m^2) of PSW-T50 panels (nos. 4 and 5) were higher than the standard, and thus met the requirements, although they could not be exactly compared. According to the JAS for structural panels[22] for reference, the standard MOE value depends on the thickness of the specimen. Class 1 requires MOE values of approximately 0.24 and 0.030 GN/m^2 for panels with thicknesses of 0.05 and 0.1 m, respectively. The E_L values of all the PSW-T100, PSW-T50, and MSW-T100 panels were higher than the standard value for the respective thickness, although they could not be exactly compared.

The MOE value of PW in the parallel direction and that of MDF were substituted into E_f in Eq. 6 for the simulation of the E_T values. The averaged MOE values of FB at the board densities of 280, 360, and 460 kg/m^3 were 0.21, 0.51, and 1.1 GN/m^2, respectively. A regression curve ($y = 2.64 \times 10^{-9} x^{3.23}$, $R^2 = 0.99$) was drawn for the MOE data of FB in Fig. 3, which approximated the data well. According to the curve, the E_{FB} values at the same densities of FB (ρ_{FB}) as the core material (ρ_c) were evaluated, which were substituted into E_c in Eq. 6 for the simulation.

The simulation results are shown in Table 3. The E_T/E_0 ratios were generally close to 1 for the PSW-T100, PSW-T50, and MSW-T100 panels. The calculated E_T values were similar to the experimental E_0 values. There was a tendency for the E_T values of PSW-T100 and PSW-T50 to be higher than the E_0 values, and the E_T value for MSW-T100 was lower than the E_0 value. As a result, the E_0 values of sandwich panels were simulated by using the E_T values from the MOE data of PW, MDF, and FB.

The improvement of MOE by sandwiching fiberboard with face materials was also estimated by considering the E_T/E_{FB} ratios at the same density of ρ_{FB} (Table 3). The E_T values of PSW-T100, PSW-T50, and MSW-T100 were approximately 10–40, 15–20, and 4 times the E_{FB} values, respectively. For example, the E_T value of PSW-T100 (6.3 GN/m^2) at a density of 430 kg/m^3 (at a core density of 390 kg/m^3) was approximately 10 times the E_{FB} value (0.62 GN/m^2) at a density of 390 kg/m^3. Higher improvement effects were estimated at a lower density.

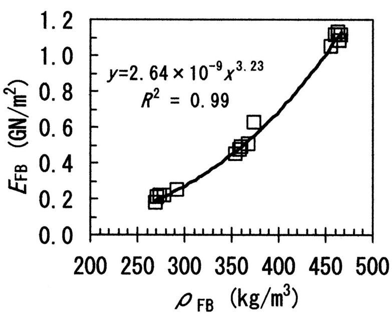

Fig. 3. Evaluation of modulus of elasticity (MOE) of fiberboard (E_{FB}) values in the simulation by the composite theory according to the regression curve drawn for the MOE data of fiberboard (FB) (*open squares*) in relation to the board density of FB (ρ_{FB})

Optimum design analysis on stiffness

Equation 4 for deflection δ_L, which is the sum of the bending and shear components, is generalized as Eq. 7:

$$\delta_L = \frac{PL^3}{B_1 E_0 I} + \frac{PL}{B_2 G_b A} \tag{7}$$

where the B_1 and B_2 are constants that depend on the geometry of bending; the constants for a four-point bending beam are $B_1 = 1296/23$ and $B_2 = 6/\kappa = 5$ (where κ is 1.2). We wish to minimize the weight of the beam for a given bending stiffness (P/δ_L). The faces are always much thinner than the core so that $f + c \approx c$, where f is face thickness. To good approximations,[3,9] when G_c is shear modulus of core material,

$$E_0 I \approx \frac{E_f b f c^2}{2} \tag{8}$$

$$G_b A \approx G_c b c \tag{9}$$

Using Eqs. 7, 8, and 9, the compliance of the beam is

$$\frac{\delta_L}{P} = \frac{2L^3}{B_1 E_f b f c^2} + \frac{L}{B_2 G_c b c} \tag{10}$$

Table 3. Parameters and results for E_0 simulation based on the composite theory

No.	Model	ρ_{FB} (kg/m^3)	E_{FB}[a] (GN/m^2)	E_f (GN/m^2)	E_T (GN/m^2)	E_T/E_0	E_T/E_{FB}
1	PSW-T100	250	0.15	13	6.0	1.18	40
2		300	0.26	13	6.1	0.99	23
3		390	0.62	13	6.3	1.15	10
4	PSW-T50	350	0.44	13	9.2	1.14	21
5		400	0.67	13	10.3	1.32	15
6	MSW-T100	330	0.36	3.0	1.6	0.89	4.4

ρ_{FB}, Density of fiberboard (FB); E_{FB}, modulus of elasticity (MOE) of FB; E_f, MOE of parallel PW (nos. 1–5) and MDF (no. 6); E_T, simulated elastic modulus of sandwich panel; E_0, experimental pure elastic modulus of sandwich panel

[a] Value of E_{FB} is substituted into E_c in the calculation (Eq. 6)

The objective function, which is the equation to be minimized in optimization theory, is the weight (W) in this case:

$$W = 2\rho_f bLf + \rho_c bLc \tag{11}$$

The dimensions b and L, the face density ρ_f, and the stiffness are fixed; the free variables are the face thickness (f), the core thickness (c), and the core density (ρ_c). If the core density (ρ_c) is fixed, the weight (W) is simply differentiated with respect to c (Eq. 13), into which the solved Eq. 10 for f is substituted (Eq. 12).

$$W = \frac{\dfrac{4\rho_f L^4}{B_1 E_f}}{c\left(c\dfrac{\delta_L}{P} - \dfrac{L}{B_2 bG_c}\right)} + c\rho_c bL \tag{12}$$

$$\frac{dW}{dc} = -\frac{\dfrac{4\rho_f L^4}{B_1 E_f}\left(\dfrac{\delta_L}{P}\right)}{c\left(c\dfrac{\delta_L}{P} - \dfrac{L}{B_2 bG_c}\right)^2} - \frac{\dfrac{4\rho_f L^4}{B_1 E_f}}{c^2\left(c\dfrac{\delta_L}{P} - \dfrac{L}{B_2 bG_c}\right)} + \rho_c bL \tag{13}$$

Setting dW/dc equal to zero in Eq. 13 gives the optimum core thickness (c_{opt}), and substituting this back into Eq. 10 gives the optimum face thickness (f_{opt}), where the plot of Eq. 12 draws a downward convex curve at $W > 0$ and $c > 0$.

Therefore, this procedure of calculation was applied to investigate of the optimum design of some virtual plywood-faced and MDF-faced sandwich panels with fiberboard. Six patterns of virtual sandwich beams were proposed and the optimum design point was analyzed for each pattern. The geometric parameters were fixed at b = 0.05 m, L = 1.5 m, L_s = 0.5 m, B_1 = 1296/23, and B_2 = 5. The material parameters that enter the analysis are listed in Table 4. The ρ_c and ρ_f were set the same as those of the manufactured sandwich panels (see Table 1). The G_c values were approximated using the G_b values of the manufactured panels because Eq. 9 gives $G_c \approx G_b$ for thin faces. The G_f values were from the MOE data of parallel PW and MDF. The P/δ_L values were set by considering the results of the manufactured panels (see Table 2). As a result, a solution for c_{opt} was obtained for each pattern under the conditions of $W > 0$ and $c > 0$.

Additionally, the optimum design point is graphically given as the point of contact in the following relationships between the two variables of the problem, f/L and c/L (Eqs. 14 and 15). The stiffness constraint (Eq. 10) gives a relationship:

$$\frac{f}{L} = \frac{2B_2}{B_1}\frac{G_c}{E_f\left(\dfrac{c}{L}\right)}\frac{1}{\left\{B_2 bG_c\left(\dfrac{\delta_L}{P}\right)\left(\dfrac{c}{L}\right) - 1\right\}} \tag{14}$$

Equation 11 gives a second relationship:

$$\frac{f}{L} = \frac{W}{2bL^2\rho_f} - \frac{\rho_c}{2\rho_f}\left(\frac{c}{L}\right) \tag{15}$$

Therefore, graphical analysis was applied to each pattern and the optimum design point was identified, as illustrated in Fig. 4.

Table 5 shows the results of the analysis on the optimum design point of each virtual sandwich beam. Judging from the ratios of c_{opt}/c and f_{opt}/f, each optimum design point was generally not far from the corresponding manufactured-panel design. Among these analysis patterns, both ratios c_{opt}/c and f_{opt}/f were closest to 1 in pattern no. 3′: the optimum core and face thicknesses were 82 and 9.9 mm, respectively. Therefore, the manufactured panel (no. 3) had the most effective structure for the weight. In the other pat-

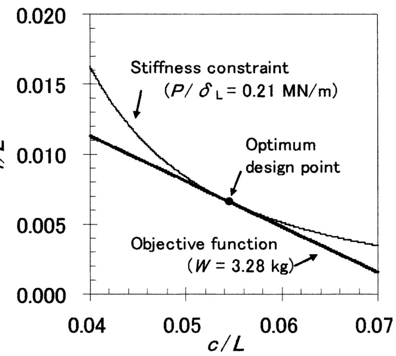

Fig. 4. Graphical analysis for the optimum design point of a virtual sandwich beam for pattern no. 3′ (see Table 4). The *curve* shows the stiffness constraint (Eq. 14) at P/δ_L = 0.21 MN/m: points that lie to the right of this curve satisfy the constraint. The optimum design point, which defines the structure with the minimum weight, is at the point where the curve and the line of the objective function (Eq. 15) come into contact. The *thick line* at W = 3.28 kg contacts the thin curve. Plywood faces with ρ_f = 600 kg/m^3, and E_f = 13 GN/m^2; fiberboard core with ρ_c = 390 kg/m^3, and G_c = 0.038 GN/m^2. Beam width b = 0.05 m, span L = 1.5 m, two-concentrated load in four-point bending at B_1 = 1296/23 and B_2 = 5

Table 4. Material parameters of virtual sandwich beams

No.	Face	ρ_c (kg/m^3)	ρ_f (kg/m^3)	G_c (GN/m^2)	E_f (GN/m^2)	P/δ_L (MN/m)
1′	PW	250	600	0.0060	13	0.071
2′		300	600	0.022	13	0.18
3′		390	600	0.038	13	0.21
4′		350	600	0.036	13	0.067
5′		400	600	0.114	13	0.042
6′	MDF	330	700	0.026	3.0	0.086

G_c, shear modulus of core material; Beam width b = 0.05 m, span L = 1.5 m, two-concentrated load in four-point bend at B_1 = 1296/23 and B_2 = 5

Table 5. Optimum design points of the virtual sandwich beams

No.	Face	ρ_{SWopt} (kg/m^3)	c_{opt} (m)	f_{opt} (m)	h_{opt} (m)	W_{opt} (kg)	c_{opt}/c	f_{opt}/f	h_{opt}/h	W_{opt}/W
1′	PW	280	0.100	0.0046	0.109	2.29	1.28	0.52	1.14	0.97
2′		340	0.095	0.0077	0.110	2.83	1.23	0.86	1.16	1.08
3′		430	0.082	0.0099	0.102	3.28	1.06	1.10	1.07	1.00
4′		400	0.050	0.0064	0.063	1.89	1.43	0.71	1.18	1.03
5′		450	0.037	0.0060	0.049	1.66	1.43	0.67	1.13	0.99
6′	MDF	390	0.094	0.0098	0.114	3.36	1.22	1.09	1.19	1.20

Optimum core thickness (c_{opt}) and optimum face thickness (f_{opt}) were calculated by setting $dW/dc = 0$ (see Eq. 13). From these thicknesses, panel density ($\rho_{SW\,opt}$), panel thickness (h_{opt}), and weight (W_{opt}) at the optimum point were calculated. The results were compared with the data of the manufactured panels in ratios to c, f, h, and W (see Table 1)

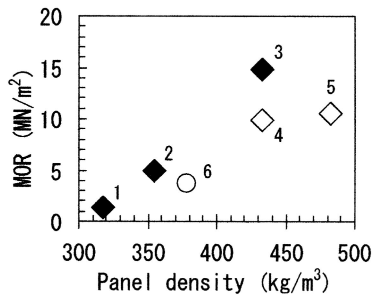

Fig. 5. Modulus of rupture (*MOR*) values of the sandwich beams in relation to panel density. *Numbers*, see Fig. 2

terns, there were tendencies that the c_{opt}/c values were more than 1, and that the f_{opt}/f values were generally less than 1. This meant that thicker core and thinner face, resulting in thicker panel thickness, should be generally desired for optimized manufacturing. The W_{opt}/W ratios were approximately 1, and were not always less than 1 due to a calculation error. The optimization was generally well applied to the wood-based sandwich panels.

Other properties

MOR values generally depended on panel density (Fig. 5). The MOR values of PSW-T100 (nos. 1, 2, and 3) were 1.3, 5.0, and 15 MN/m^2, respectively, and those of PSW-T50 (nos. 4 and 5) were 9.8 and 11 MN/m^2, respectively. The thicker PSW-T100 panel (no. 3) was somewhat advantageous in MOR over the PSW-T50 panel (no. 4) at the same panel density (430 kg/m^3), while in contrast, the reverse trend was observed in the E_L values of these panels (Fig. 2B). The MOR for MSW-T100 was 3.7 MN/m^2.

For reference, all of the MOR values of the sandwich panels met the requirements in the JAS standard[22] for Class 1 that requires the panels with thicknesses of 0.05 and 0.1 m to provide the MOR values of approximately 2.8 and 0.71 MN/m^2, respectively.

The average MOR of PW with a density of 600 kg/m^3 in the parallel direction was 96 MN/m^2 (that in the perpendicular direction was 18 MN/m^2). The average MOR of MDF with a density of 700 kg/m^3 was 33 MN/m^2, which was about one third of that of PW in the parallel direction. The MOR value of PSW-T100 (no. 3) was approximately one sixth of that of PW in the parallel direction, and four times those of FB at the same density as the core density: the average MOR values of FB at densities of 280, 360, and 460 kg/m^3 were 1.6, 3.7, and 9.5 MN/m^2, respectively. The observed failure appearances of these sandwich panels were almost all shear failure that occurred in the core layer. Core shear or face yield was observed in the specimens of PSW-T100 (no. 3).

Generally, the various failure modes (face yield, core shear, face wrinkling) for sandwich structures in bending can be illustrated in a diagram in relation to design parameters: the ratio of ρ_c to raw material density and the ratio of face thickness to span (f/L).[3,23,24] The diagram is divided into fields of dominant failure modes, separated by field boundaries. On the boundary, a transition in failure mode occurs when the two modes have the same failure load, where b and c are cancelled in the calculation. There is a trend for the relation between the modes of face yield and core shear: the face yield is dominant with high ρ_c at a fixed f/L ratio, and at high f/L ratio at a fixed ρ_c; core shear is dominant in the reverse conditions.

The ρ_c was a variable in the diagram for the wood-based sandwich panels, because the f/L ratios were fixed at 0.09/1.5 in this case. ρ_c of the panel (no. 3) was relatively high. The test conditions must have been in the core shear mode for low ρ_c values, and on the border of core shear and face yield modes at higher ρ_c values. It was considered that the face yield mode would be obtained if a longer L was taken with the same face thickness and the same core density. Although the diagram in this case is required for certification, more details were omitted in this article. The optimization of both stiffness and strength, which would be useful if the strength constraint is additionally related to f/L and c/L, was also omitted here.

The bending test was a pilot-scale test using the sandwich beam specimens, and was useful for determining the elastic and shear moduli. The manufacturing capacity of this panel should be improved, and practical tests should be conducted for panels 90–120 cm in width, and 240 or 300 cm in length for their respective wall or floor uses following JIS A 1414.[19]

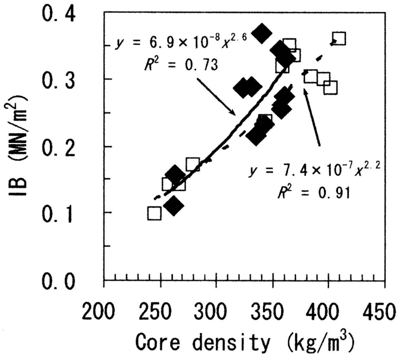

Fig. 6. Internal bond (*IB*) of PSW-T100 (*filled diamonds*) in relation to core density. The data were compared to that of FB (*open squares*). Regression curves for PSW-T100 (*solid line*) and for FB (*dotted line*) are shown

The average IB values of PSW-T100 were 0.13, 0.28, and 0.30 MN/m^2 for panel densities of 330, 390, and 400 kg/m^3 (for the core densities of 260, 340, and 360 kg/m^3), respectively. The average IB values of PSW-T100 increased with the increase of panel density. An IB of 0.3 MN/m^2 is required, according to JIS A 5908 for veneer-overlaid particleboard.[21] According to the JAS for structural panel,[22] the IB is also required to be 0.3 MN/m^2. Therefore, a panel density of at least 400 kg/m^3 (hence the core density of 360 kg/m^3) met the requirements for structural use.

As figured in relation to the core density (Fig. 6), the increasing trend in IB was similar to that of FB. Because the IB failures of PSW-T100 occurred in the core materials and the density profiles of the core materials of PSW-T100 were flat through the thickness, the IB values of PSW-T100 were considered to depend on the core densities. There was no difference in the IB properties between the steam-injection pressed PSW-T100 and the hot-pressed FB. The average IB of FB at a density of 360 kg/m^3 was 0.31 MN/m^2, similar to the lowest limit of the core density of PSW-T100 for structural use. This result was also similar to that of another low-density fiberboard,[1] which was made from softwood fibers and processed by a batch-type steam-injection pressing, where the lowest density limit was approximately 350 kg/m^3.

As shown in Fig. 7A, the TS values of the sandwich panels were in the range of 1.7%–3.0%. The TS values of all the sandwich panels were much less than the requirement for a TS value of less than 12%, according to JIS A5908.[21] There was a trend that the WA values (Fig. 7B) increased at lower density, whereas the TS values generally decreased. This was because the lower-density panels included more porosity, which absorbed more water. Due to the low compaction ratios (low core-to-fiber density ratios), dimensional stability was not significantly affected by the increase of WA.

The PSW-T100 at a panel density of 430 kg/m^3 provided the TS value of 2.1% and WA of 17% on average. From the above results, the PSW-T100 at a panel density of more than 400 kg/m^3, which met the requirements for IB for structural use, provided excellent dimensional stability in TS.

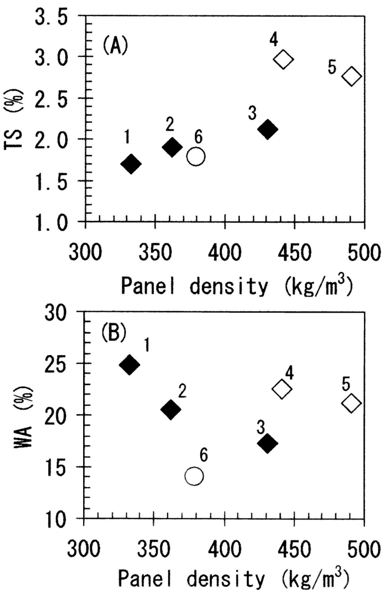

Fig. 7A,B. Thickness swelling (*TS*) (**A**) and water absorption (*WA*) (**B**) of the sandwich panels in relation to panel density. *Numbers*, see Fig. 2

Conclusions

Several wood-based sandwich panels with low-density fiberboard were manufactured for structural insulated walls/floors, and the elastic moduli in four-point out-plane bending and other fundamental properties were evaluated. Because the density control was critical for structural insulation use of panel, optimum design analysis on stiffness was well applied to wood-based sandwich panels in four-point bending.

As a result, the PSW-T100 at a density of 430 kg/m^3 (no. 3) had the most effective structure for improving $E_L I$ (13×10^{-6} GNm^2) (where the E_L, E_0, and G_b were 3.5, 5.5, and 0.038 GN/m^2, respectively) among these panels, and met the requirements for structural use with an excellent dimensional stability. Its structure was found to be the optimum design to provide the stiffness with minimum weight based on the analysis. The panel (no. 3) has also been advantageous for both steady-state and non-steady-state insulations due to an adequate low density and a sufficient panel thickness.[8]

Therefore, it was concluded that the PSW-T100 panel (no. 3) was the most feasible as a structural insulated wall/floor. The practical use of PSW-T100 as a structural insulated wall/floor is expected to improve the energy efficiency of indoor environments, and make them more comfortable to live and work in.

Acknowledgments The authors thank Mr. Noritoshi Sawada and his cooperative members (Hokushin) for technical support in the manufacturing of the sandwich panels. We also thank Drs. Kenji Umemura, Wong Ee Ding, and Guangping Han for their help and advice in manufacturing the panels. We are grateful to Hokushin for the fiber, adhesive, and MDF, to Ishinomaki Plywood for the plywood, and to Gun-ei Chemical for the adhesive.

References

1. Kawasaki T, Zhang M, Kawai S (1998) Manufacture and properties of ultra-low density fiberboard. J Wood Sci 44:354–360
2. Structural Board Association (2000) OSB performance by design – OSB in wood frame construction (Canadian edition). Structural Board Association, Ontario
3. Gibson LJ, Ashby MF (1997) The design of sandwich panels with foam cores. In: Clarke DR, Suresh S, Ward FRSIM (eds) Cellular solids. Cambridge University Press, Cambridge, pp 345–386
4. Wang Q, Sasaki H, Yang P, Kawai S (1992) Utilization of laminated-veneer-lumber from Sabah plantation thinnings as beam flanges. III. Production of composite beam and its properties. Mokuzai Gakkaishi 38:914–922
5. Zhang M, Kawasaki T, Yang P, Honda T, Kawai S (1996) Manufacture and properties of composite fiberboard III. Properties of three-layered bamboo–wood composite boards and stress analysis by the Finite Element Method. Mokuzai Gakkaishi 42:854–861
6. Kawasaki T, Zhang M, Kawai S (1999) Sandwich panel of veneer-overlaid low-density fiberboard. J Wood Sci 45:291–298
7. Kawasaki T, Kwang H, Komatsu K, Kawai S (2003) In-plane shear properties of the wood-based sandwich panels as a small shear wall, evaluated by the shear test method using tie-rods. J Wood Sci 49:199–209
8. Kawasaki T, Kawai S (2006) Thermal insulation properties of wood-based sandwich panel for use as structural insulated walls ans floors. J Wood Sci 52:75–83
9. Allen HG (1969) Analysis and design of structural sandwich panels. Pergamon, Oxford
10. Arima T, Okuma M (1970) Studies on compound used injected and foamed polyurethane resin as core. I (in Japanese). Mokuzai Kogyo 25:267–268
11. Okuma M, Arima T (1970) Studies on compound used injected and foamed polyurethane resin as core. II (in Japanese). Mokuzai Kogyo 25:418–420
12. Vinson JR (1999) The behavior of sandwich structures of isotropic and composite materials. Technomic, Pennsylvania
13. Carlson LA, Nordstrand T, Westerlind B (2001) On the elastic stiffness of corrugated core sandwich. J Sandw Struct Mater 3:253–267
14. Whitney JM (2001) A local model for bending of weak core sandwich plates. J Sandw Struct Mater 3:269–288
15. Swanson SR, Kim J (2002) Optimization of sandwich beams for concentrated loads. J Sandw Struct Mater 4:273–293
16. Gupta N, Woldesenbet E, Kishore, Sankaran S (2002) Response of syntactic foam core sandwich structured composites to three-point bending. J Sandw Struct Mater 4:249–272
17. JAS (2000) JAS for structural plywood, Ministry of Agriculture, Forestry and Fisheries, Tokyo
18. Sasaki H (1991) Development of continuous press with steam-injection heating from both sides. Report for the Grant-in-Aid for Scientific Research (No. 01860023) from the Ministry of Education, Science and Culture of Japan
19. JIS (1994) JIS A 1414 Methods of performance test of panels for building construction. Japanese Standard Association, Tokyo
20. JIS (2003) JIS A 5905 Fiberboards. Japanese Standard Association, Tokyo
21. JIS (2003) JIS A 5908 Particleboards. Japanese Standard Association, Tokyo
22. JAS (2003) JAS for structural panel. Ministry of Agriculture, Forestry, and Fisheries, Tokyo
23. Triantafillou TC, Gibson LJ (1987) Failure mode maps for foam core sandwich beams. Mat Sci Eng 95:37–53
24. Triantafillou TC, Gibson LJ (1987) Minimum weight design of foam core sandwich panels for a given strength. Mat Sci Eng 95:55–62